"Physics of Auroral Phenomena", Proc. XXX Annual Seminar, Apatity, pp. 133 - 136, 2007

Polar Geophysical Institute

MAGNETIC FIELD DYNAMICS ABOVE THE ACTIVE REGION AR 0365 IN PREFLARE STATE

A.I. Podgorny[1], I.M. Podgorny[2], N.S. Meshalkina[3]

[1]*Lebedev Physical Institute RAS, Moscow, Russia podgorny@fian.fiandns.mipt.ru,*
[2]*Institute for Astronomy RAS, Moscow, Russia, podgorny@inasan.ru*
[3]*Institute for Solar-Terrestrial Physics SO RAS, Irkutsk, Russia, nata@iszf.irk.ru*

Abstract. MHD simulations in the solar corona above the active region AR 0365 with the large domain (4×10^{10} cm) snow that emergency of the new magnetic flux from-under the photosphere is accompanied by sequentially appearing of several current sheets (CS). Each of CS can produce one of the observed elementary flares.

Introduction

The primordial energy release takes place high in the solar corona on the height about 3×10^9 cm, up to 10^{10} cm. Now it is proved by high-resolution hard X-ray observations on the limb of the Sun [1]. This can be explained by energy accumulation in the magnetic field of CS in the solar corona above an active region. The CS instability causes the explosive energy release with all observational manifestations as CME appearance, flare emission, and particle acceleration explained by electrodynamical model of the solar flare [2].

The problem is to perform MHD simulation of CS creation in the magnetic field of corona for a real active region. CS cannot be observed directly, because 3D magnetic field configuration in the corona cannot be obtained from measurements. The observations make possible to find only the magnetic field distribution on the photosphere. The simulation for a real active region means that all the conditions for simulation are taken from observations before the flare. The magnetic field distribution observed on the photosphere should be used for setting boundary conditions. It should be emphasized that in such simulations it is not assumed any solar flare mechanism. Here the attempt to prove the solar flare mechanism, which is based on CS creation, is present. But such a simulation can also reveal any other mechanism, if it should be really responsible for solar flare.

For the fist step of simulations in the active region of the solar corona, magnetic field approximation by the field of several magnetic dipoles has been used [3, 4]. The MHD simulations show CS creation in the vicinity of singular line and permit to find magnetic field energy of the sheet. But such approximation does not take into account some singularities and other important details of the field configuration. For more precise simulation [5, 6] the observed magnetic field distribution on the photosphere is used directly for setting boundary conditions and initial potential magnetic field is calculated. In [5] for the large active region with the size ~ 2.5×10^{10} cm, which has been produced Bastille flare, too rough numerical greed is used. These simulations show only tendency to CS creation. In [6] the simulations are performed for active region AR 0365 with the size ~ 10^{10} cm. The flare position found from MHD simulations as position of CS is coincide well with the position of the maximum of radio-emission intensity measured with the Siberian Solar Radio Telescope (SSRT, Irkutsk) on wave length 5.2 cm. Such coincidence supports the mechanism of the solar flare based on CS creation. These simulations are performed in the region with the size 1.2×10^{10} cm. The potential field in the corona for such approximation does not contain all X-type singularities of the real magnetic field. To take into account all X-type singularities the region with the size 4×10^{10} cm is used. The first results of simulation in a such large region are presented in this work.

Equations and conditions for simulation

The simulations are performed by numerical solving of 3D MHD equations above the active region of the solar corona. Its lower boundary is situated on the photosphere and contains the active region AR 0365. The calculations are done in the computational domain ($0\le x\le 1$, $0\le y\le 0.3$, $0\le z\le 1$, in dimensionless units). The unit of the length is chosen as the size of photospheric boundary of the computational domain $L_0=4\times10^{10}$ cm. The Y-axis is directed away from the Sun normally to the photosphere. The XZ (y=0) plane is the photospheric plane. The X-axis is directed from East to West, and the Z-axis is directed from North to South. Situation of photospheric boundary of the computational domain (y=0, $0\le x\le 1$, $0\le z\le 1$) in the flare day 27 May 2003 is shown in Fig. 1a. The unit of the magnetic field B_0=300 Gauss is taken. The dimensionless units of plasma density and temperature are taken to be equal to their values in the initial moment of time in the corona, which are supposed to be constant in space $\rho_0=10^8$ cm^{-3}, $T_0=10^6$ ^oK. The dimensionless units of the plasma velocity, time, and the current density are taken as correspondingly the Alfvenic velocity $V_0 = V_A = B_0/\sqrt{4\pi\rho_0}$, $t_0 = L_0/V_0$, $j_0 = cB_0/4\pi L_0$. The 3D dimensionless MHD equations have a form:

$$\frac{\partial \mathbf{B}}{\partial t} = \mathrm{rot}(\mathbf{V}\times\mathbf{B}) - \frac{1}{\mathrm{Re}_m}\mathrm{rot}\left(\frac{\sigma_0}{\sigma}\mathrm{rot}\mathbf{B}\right) \quad (1)$$

$$\frac{\partial \rho}{\partial t} = -\mathrm{div}(\mathbf{V}\rho) \quad (2)$$

$$\frac{\partial \mathbf{V}}{\partial t} = -(\mathbf{V},\nabla)\mathbf{V} - \frac{\beta_0}{2\rho}\nabla(\rho T) - \frac{1}{\rho}\left(\mathbf{B}\times\mathrm{rot}\mathbf{B}\right) + \frac{1}{\mathrm{Re}\rho}\Delta\mathbf{V} + G_g\mathbf{G} \quad (3)$$

$$\frac{\partial T}{\partial t} = -(\mathbf{V},\nabla)T - (\gamma-1)T\mathrm{div}\mathbf{V} + (\gamma-1)\frac{2\sigma_0}{\mathrm{Re}_m\sigma\beta_0\rho}\left(\mathrm{rot}\mathbf{B}\right)^2 - (\gamma-1)G_q\rho L'(T) +$$

$$+\frac{\gamma-1}{\rho}\mathrm{div}\left(\mathbf{e}_{\parallel}\kappa_{dl}(\mathbf{e}_{\parallel},\nabla T) + \mathbf{e}_{\perp 1}\kappa_{\perp dl}(\mathbf{e}_{\perp 1},\nabla T) + \mathbf{e}_{\perp 2}\kappa_{\perp dl}(\mathbf{e}_{\perp 2},\nabla T)\right) \quad (4)$$

The restrictions connected with the finite step of the difference scheme do not permit to set real dimensionless parameters, which characterize the diffusion terms of equations (1)-(4). The principle of limited simulation (Podgorny, 1978) [7] is used. According to this principle, the dimensionless parameters, which are much larger then 1 should be chosen larger than 1 in the numerical experiment, but their order of magnitude can be different. In our calculations the parameters are chosen as $\gamma = 5/3$, $\mathrm{Re_m}=1000$, $\mathrm{Re}=300$, $\beta=0.6\times10^{-5}$, $\Pi=100$, $\Pi_B=10^4$, $G_q=0.3\times10^{-5}$. The gravitation force can be neglected comparing with magnetic and plasma pressure forces: $G_g=0$.

According to [8] the flare appears one or two days after the magnetic flux emergency from-under the photosphere. The numerical solving of MHD equations is initiated three days before the flare, when there are no strong disturbances and the magnetic field in the active region of the solar corona can be considered as potential one. The potential magnetic field is found by solving of Laplace equation for the magnetic potential φ_B ($\mathbf{B}=-\nabla\varphi_B$) with the inclined derivative along the line-of-sight as the boundary condition on the photospheric boundary:

$$\Delta\varphi=0; \quad \partial\varphi/\partial l_{\mathrm{sight}}|_{\mathrm{PhBoun}} = -B_{\mathrm{lsight}}; \quad \mathbf{B}=-\nabla\varphi \quad (5)$$

The distribution of the line-of-sight magnetic field component B_{lsight} on the photosphere is taken from magnetic maps observed by SOHO MDI (http://soi.stanford.edu/magnetic/index5.html).

To solve the system of MHD equations it is need to set two magnetic field components parallel to the boundary on the photospheric boundary of the domain in each moment of time. But SOHO MDI observes on the photosphere only line-of-sight magnetic field component. For setting boundary conditions, two parallel to the photosphere magnetic field components are taken from calculated potential magnetic field by solving of the equation (5) by the same way as for initial moment of time. Such method is valid because the magnetic field on the photosphere is defined mainly by the currents under the photosphere, but not by the currents in corona.

To stabilize the instabilities several methods are used. It is used an absolutely implicit finite-difference scheme, which is solved by the iteration method [9]. The scheme is also conservative relative to the magnetic flux. The artificial viscosity is introduced near the computational domain boundary, and some other special methods are used.

Results of simulation

The potential magnetic field calculated for observed line-of-sight magnetic field distributions on the photosphere in the flare day on 27 May 2003 is shown in Fig. 1. The potential field configurations are presented in the perpendicular to the photosphere planes that intersects the photosphere through the lines shown in the Fig. 1. It can be seen X-type field singularities in these planes.

The configurations of the calculated potential magnetic field in the central plane of region ($z=0.5$) are represented in Fig. 2. This plane is the most representative. It contains all main singularities. The calculations is obtained for the sizes of photospheric boundaries of computational domains equal to $L_0=2\times10^{10}$, $L_0=4\times10^{10}$, and $L_0=6\times10^{10}$. This figure explains, why it is necessary to choose the size of the region equal $L_0=4\times10^{10}$. The configurations for the region with the size $L_0=4\times10^{10}$ is practically the same as for one with the size $L_0=6\times10^{10}$. The configuration for the region with the size $L_0=2\times10^{10}$ is somewhere different comparing with one with the size $L_0=4\times10^{10}$: one of the X-type singularities is absent, another singularity is rather deformed.

The evolution in time of the magnetic field configuration in the central plane ($z=0.5$) is shown in Fig. 3. The disturbances propagate from the photosphere up to the corona. Under the action of these disturbances, the magnetic field near the X-type points is deformed into configuration of CS. It should be emphasized that emergency of a new magnetic flux from-under the photosphere, accompanied by CS creation near the already existing singular lines, causes a new X-type singularities appearing. CS is created in its vicinities. Several such X-points with CS sequentially emerge from-under the photosphere (see Fig. 3) and moves leftward. Then all these X-points disappear except the last one. The last emerged X-point continues to exist all remaining time of calculation, but CS in its vicinity disappears due to field dissipation. The dynamic of the magnetic field with such motion of CS is seen in the big domain. It is not observed for simulations in computational domain with the size 1.2×10^{10} cm [6]. Probably, the reason of this effect is the magnetic field setting on the adjoining to the photosphere nonphotospheric boundaries,

which are situated not very far from the region of the large field. It does not permit to change the magnetic field inside the region in very free manner.

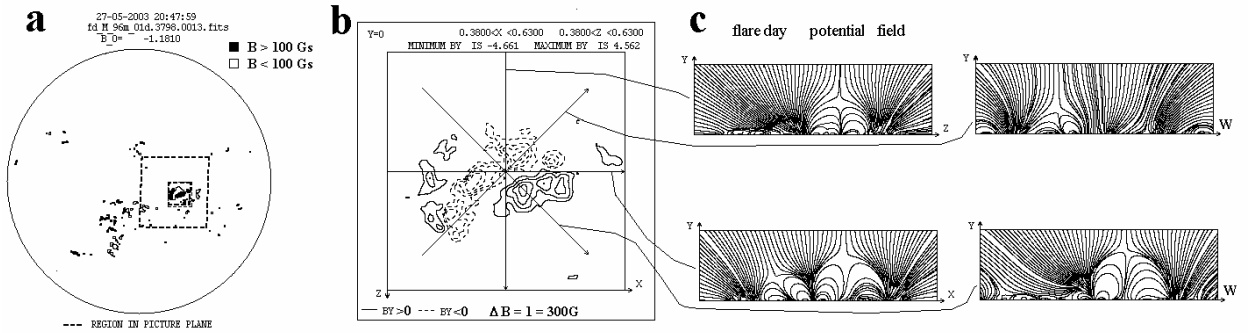

Figure 1. (a) - SOHO MDI magnetic maps on solar disk in the flare day 27 May, 2003. The position of the photospheric boundary of the computation domain on the disk and position of regions of isolines of normal to the photosphere calculated potential magnetic field component, which is shown in (b). (c) - the magnetic field configurations in the planes perpendicular to the photosphere,. The intersections of these planes with the photosphere are shown in (b).

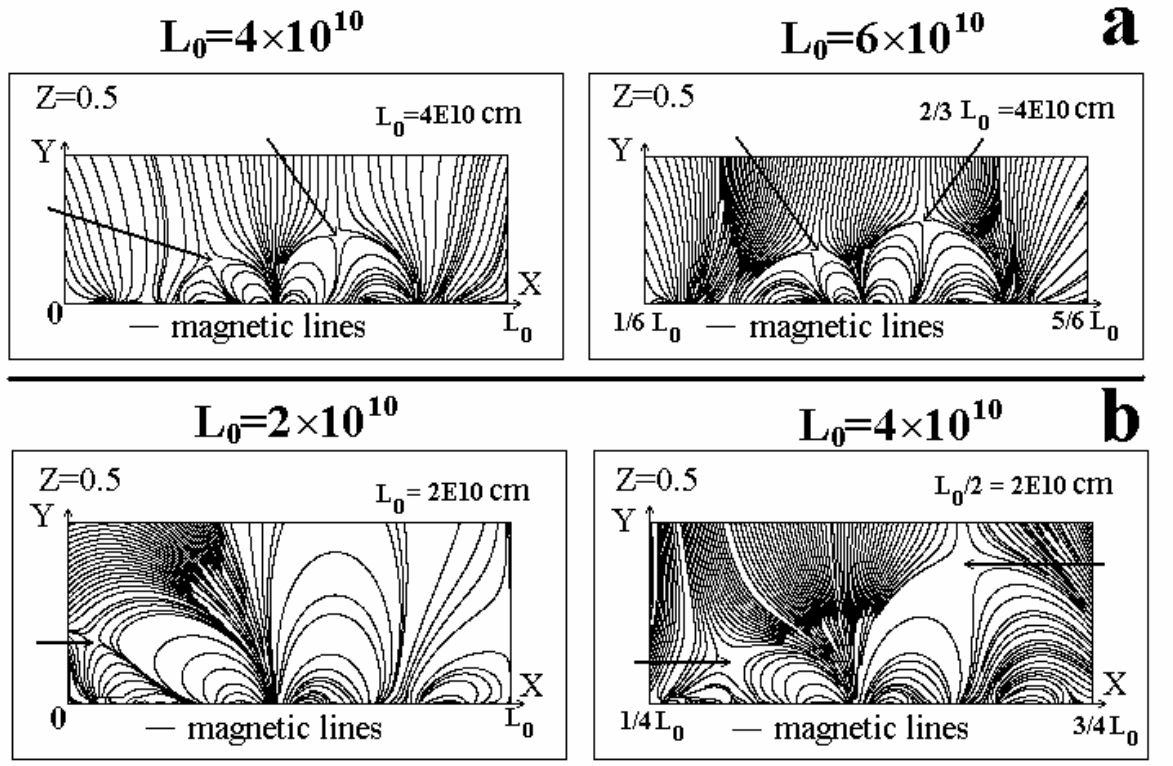

Figure 2. Comparison of calculated potential magnetic field configuration in the central plane z=0.5 for region sizes $L_0=6\times10^{10}$ cm and $L_0=4\times10^{10}$ cm (a) and $L_0=2\times10^{10}$ cm and $L_0=4\times10^{10}$ cm (b). X-type points are shown by arrows.

The flares can occur due to instability of CS appearing in each of such X-type points. But the magnetic field near the X-points emerged from-under the photosphere is much larger, then magnetic field near the already existing X-points situated higher. So more energy accumulates in CS appeared near the emerged X-points, and these CS must produce more powerful flares. The sheets appeared near the emerged X-points are almost vertical ones (see Fig. 3). The flares in these sheets can produce CME, because of the **j**×**B** force, which accelerates plasma in the sheet. It is directed away from the Sun.

It should be expected that radio and hard X-ray flare emission sources appear in CS. Other sources of flare emission are situated in the places of intersections of magnetic lines coming from CS with the photosphere. Electron acceleration takes place in the field-aligned currents according to the electrodynamic model of the flare [2]. The primary rough comparison shows approximately coincidence of these positions with positions of radio and hard X-rays flare sources obtained from observations. But the X-points in the plane z=0.5 only approximately corresponds

to real CS positions, because the lines, which pierce this points, are not exactly singular ones. The plane that intersects normally by a singular line must not be by all means perpendicular to the photosphere. Now it is necessary to find the real CS positions, using methods developed in [6], and to perform accurately the comparison with observations. Also in future for improving of solar flare prognosis it is necessary to modernize the numerical methods and to use supercomputers to accelerate calculations.

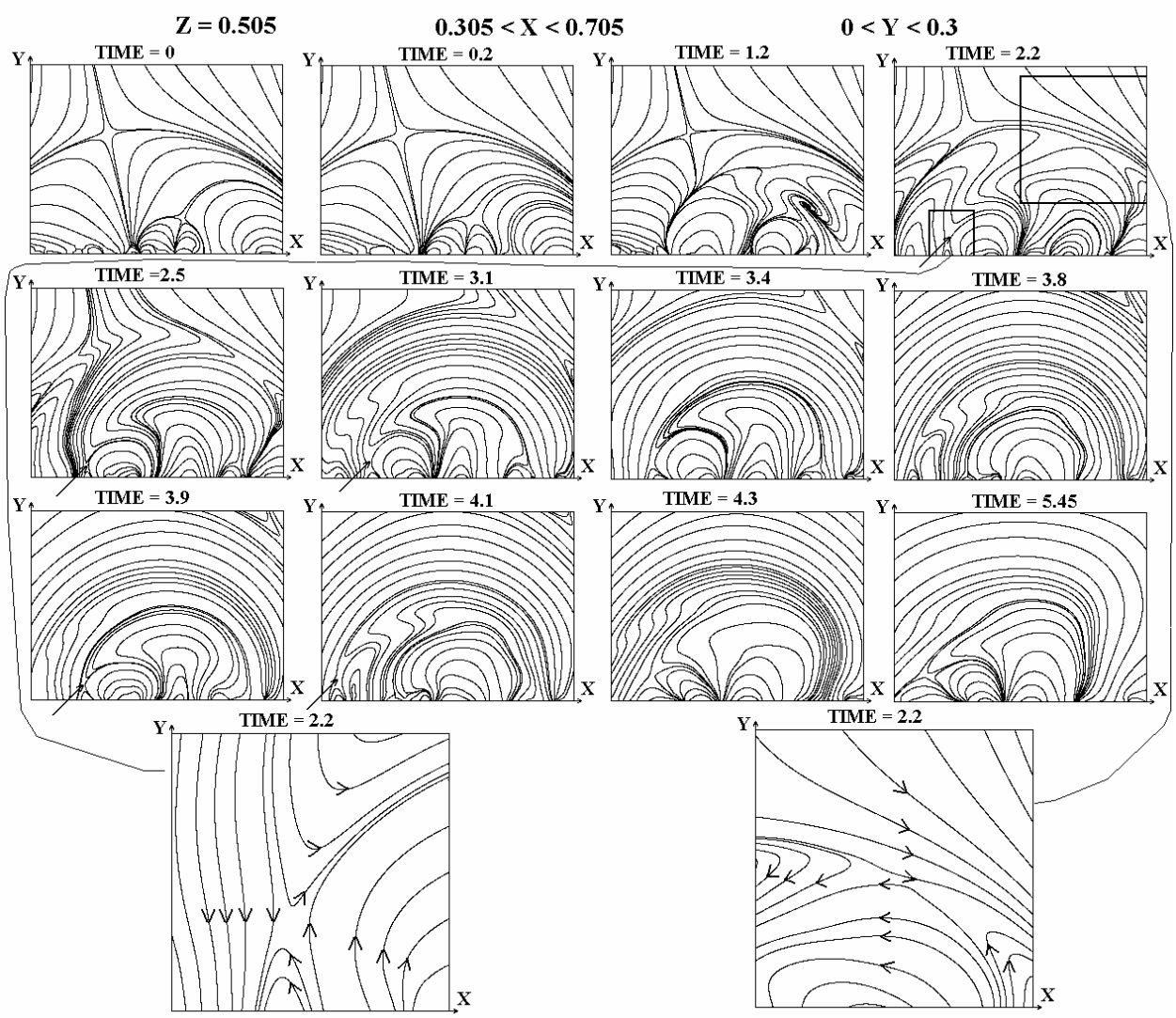

Figure 3. Evolution of the magnetic field configuration in the central plane z=0.5, emerged X-points with current sheets (some of them are shown by arrows). Configurations near current sheets for t=2.2 are shown in details.

Acknowledgments. This work was supported by RFBR grant № 06-02-16006.

References

1. Lin R. P., Krucker, S., Hurford, G. J., *et al.*: 2003, *Astrophys. J.* **595**, L69.
2. Podgorny, A. I. and Podgorny, I. M.: 2006, *Astronomy Report*. 50, 842.
3. Bilenko I. A., Podgorny A. I., Podgorny I. M.: 2002, *Solar Phys.* **207,** 323.
4. Podgorny A. I., Podgorny I. M.: 2003, Proc. Physics of 26 Annual Seminar. Apatity. P. 151.
5. Podgorny A. I., Podgorny I. M.: 2004, Proc. Physics of 27 Annual Seminar. Apatity. P. 87.
6. Podgorny A. I., Podgorny I. M, Meshalkina N. S.: 2006: Proc. Physics of 29 Annual Seminar. Apatity. P. 203.
7. Podgorny I. M.: 1978, *Fund. Cosmic Phys.* **1**, 1.
8. Ishkov V. N.: 2001 *Astron. Astroph. Trans.* **20**, 563.
9. Podgorny A. I. and Podgorny I. M.: 2004: *Comput. Mathematics and Mathemat. Physics*. **44**, 1784.